SPECIAL TOPIC
Monitoring China's Environmental Change with Remote Sensing

August 2012 Vol.57 No.22: 2865–2871
doi: 10.1007/s11434-012-5099-x

Changes in tropospheric ozone levels over the Three Representative Regions of China observed from space by the Tropospheric Emission Spectrometer (TES), 2005–2010

SHEN LuLu & WANG YuXuan*

Ministry of Education Key Laboratory for Earth System Modeling, Center for Earth System Science, Institute for Global Change Studies, Tsinghua University, Beijing 100084, China

Received December 15, 2011; accepted February 16, 2012; published online April 24, 2012

Tropospheric ozone observations over China from 2005 to 2010 at three pressure levels (484, 681 and 825 hPa) from the Tropospheric Emission Spectrometer on board the NASA Aura satellite have been analyzed. Fourier Transform analysis revealed the trends and seasonality of regionally-averaged, monthly-mean ozone concentrations over western, northern and southern China. Significant increases in ozone levels are found over all three regions at 464 hPa and the rate of increase is fastest over northern China, reaching 0.89 ± 0.059 nL/(L a). At 681 hPa, ozone shows increases over northern and western China, at a rate of 0.57 ± 0.065 nL/(L a) and 0.41 ± 0.041 nL/(L a) respectively, but is constant over southern China. At 825 hPa, ozone increases at a rate of 0.36 ± 0.074 nL/(L a) over northern China, while decreasing over southern China at a rate of -0.21 ± 0.061 nL/(L a). Over the three regions, ozone levels are generally higher in summer and lower in winter. Over southern China at all three pressure levels and northern China at the 825 hPa level, ozone shows double peaks occurring in spring and autumn as a result of the combined effects of atmospheric chemistry and global transport. This work provides a useful observational dataset and tools for future analysis of changes in tropospheric ozone over China.

TES, ozone, China, interannual variation, seasonal variation

Citation: Shen L L, Wang Y X. Changes in tropospheric ozone levels over the Three Representative Regions of China observed from space by the Tropospheric Emission Spectrometer (TES), 2005–2010. Chin Sci Bull, 2012, 57: 2865–2871, doi: 10.1007/s11434-012-5099-x

Ozone is an important greenhouse gas and major precursor of the hydroxyl radical (OH) in the troposphere. Surface ozone is a pollutant, with adverse impacts on human health and vegetation. Ozone precursors include NO_x, VOCs, and CO. Compared with other gas pollutants, ozone has a relatively long lifetime (1–2 weeks in summer and 1–2 months in winter) [1], making it subject to long-range transport. Accordingly, ozone has been considered as a global pollutant, and much attention has been paid to temporal and spatial variability of tropospheric ozone, long-range transport of ozone and its precursors at both continental and hemispheric scales, and the effect of ozone on regional and global climate [2–4].

It has been suggested that tropospheric ozone concentrations have increased significantly since the Industrial Revolution, especially in the Northern Hemisphere [5]. China's rapid economic growth in recent years has resulted in fast increasing emissions of ozone precursors (NO_x, VOCs and CO). Richter et al. [6] indicated that NO_2 emissions from China have increased by 50% between 1996 and 2003 based on remote sensing data derived from GOME and SCIAMACHY satellite instruments. This is much higher than that suggested by the bottom-up inventory [7]. By analyzing the Measurement of Ozone and Water Vapor by Airbus In-Service Aircraft (MOZAIC) flight data, Ding et al. [8] found that tropospheric ozone in eastern China has increased at an annual rate of 2% during the past 10 years. Wang et al. [9] indicated that background ozone in southern

*Corresponding author (email: yxw@tsinghua.edu.cn)

© The Author(s) 2012. This article is published with open access at Springerlink.com

China has increased at a rate of 0.58 nL/(L a), based on Hong Kong surface observations from 1994 to 2007.

Since the 1980s, China has built a few continuous surface observation stations, such as those at Shangdianzi, Linan, Longfengshan and Waliguan. These generate basic data about surface ozone concentrations and seasonal variations of the different regions [10–13]. However, compared to developed countries, ozone observations in China are very limited. Satellite remote sensing of atmospheric composition is a useful complement to surface observations. Several satellite instruments are capable of providing open-access, quantitative information on atmospheric concentrations of ozone and its precursors, including the OMI (Ozone Monitoring Instrument) and the TES (Tropospheric Emission Spectrometer) [14,15]. The TES can provide vertical ozone distributions of O_3 and CO simultaneously. Since its launch in 2004, the TES has accumulated a large amount of data applicable to the relationships between ozone and precursors, as well as the intercontinental transport of ozone [7].

In this study, we examine the change in tropospheric ozone over China from 2005 to 2010 using TES generated ozone retrieval products.

1 Data and methodology

1.1 Introduction to TES data

TES is a Fourier transform infrared emission spectrometer covering the spectral range 650–2050 cm^{-1} (3.3–15.4 μm) at a spectral resolution of 0.1 cm^{-1} (nadir viewing) or 0.025 cm^{-1} [16] (limb viewing). The infrared emission and absorption of the atmospheric substances closely relate to the cloud cover, pollutant concentration, pressure, temperature and other factors. Therefore, TES is able to retrieve the vertical profile of species concentrations on the basis of the emission and absorption spectrum. The method used by TES to retrieve tropospheric profiles of ozone and CO [17] has been optimized. The retrieved profile may be expressed as a linear combination of the true profile and the *a priori* profile weighted by the averaging kernel matrix. Ozone data provided by TES usually covers a wide range from 0–32 km in altitude, including the whole troposphere and the lower part of the stratosphere. In the lower part of troposphere, there are 1–2 degrees of freedom in the inversion method used, indicating the capability of TES to observe the vertical distribution of ozone [18].

The official TES website provides open access to the retrieval products of tropospheric ozone (http://tes.jpl.nasa.gov/). This study uses the level 3 retrieval data from Sep 2004 to Dec 2010, at 3 different elevations (825, 681 and 464 hPa). As an example, Figure 1 shows the global distribution of ozone at 681 hPa in July 2009 retrieved by TES.

1.2 Methodology

The Fast Fourier transform (FFT) methodology is used to decompose the time-series into the sum of different sine and cosine functions with different amplitudes and frequencies. By filtering and the Inverse Fast Fourier Transform (IFFT), information is obtained in the desired frequency ranges. Fourier transform is widely applied in the study of inter-annual change and seasonal variations [19,20]. We define the inter-annual trend as periods longer than 1.4 years with seasonal variation less than 1.3 years. The sample frequency in this study is 12 Hz, i.e. 1 year. A frequency of 2 Hz is 6 months, 3 Hz 4 months, etc.

2 Data summary

The TES ozone time-series data is from Sep 2009 to Dec 2010 at three different pressure levels (825, 681 and 464 hPa) (Figure 2). On the TES website, China is divided into 3 geographical regions: western, northern and southern China. Due to the high elevation of western China, the TES data there at 825 hPa is scarce, so this is not included in this study. Over western and northern China, ozone mixing ratios have summer maxima and winter minima. Over southern China, however, they are higher in winter and lower in summer. At 681 and 825 hPa pressure levels, ozone over southern China shows double peaks occurring in spring and autumn. The inter-annual trend is discussed below.

As summarized in Table 1, the average ozone mixing ratio is higher over northern China than over southern China. Ozone mixing ratios increase with altitude, partly resulting from the downward transport of stratospheric ozone.

3 Regional analysis

Due to the significant differences between the different parts of China, the temporal variability of ozone is split by region.

3.1 Northern China

Figure 3 shows the frequency spectrum of ozone over

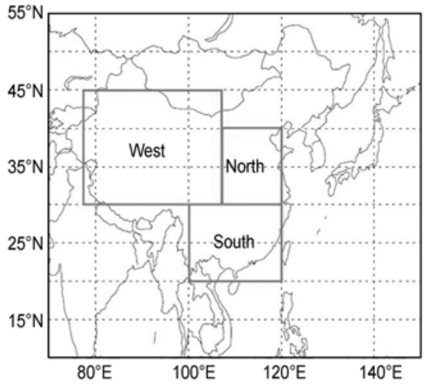

Figure 1 The three geographic regions of China adopted by TES. (http://tes.jpl.nasa.gov/visualization/SCIENCE_PLOTS/Trends/world_map_clickable.html, read 2011/10/9).

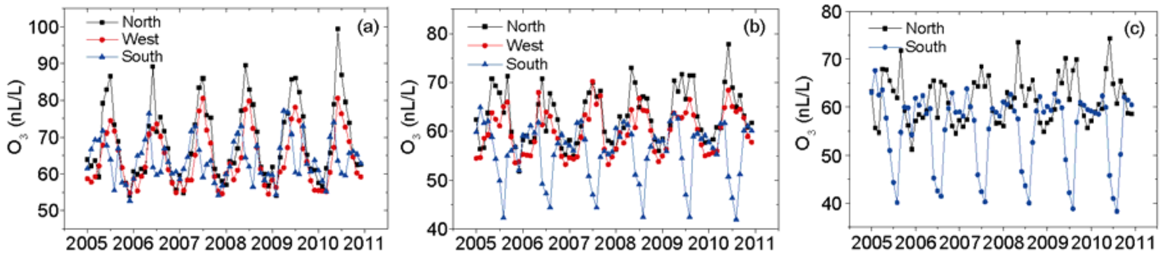

Figure 2 Ozone mixing ratios at 464 hPa (a), 681 hPa (b) and 825 hPa (c) pressure levels retrieved from the TES between 2005 and 2010 over western China (red), northern China (black), and southern China (blue).

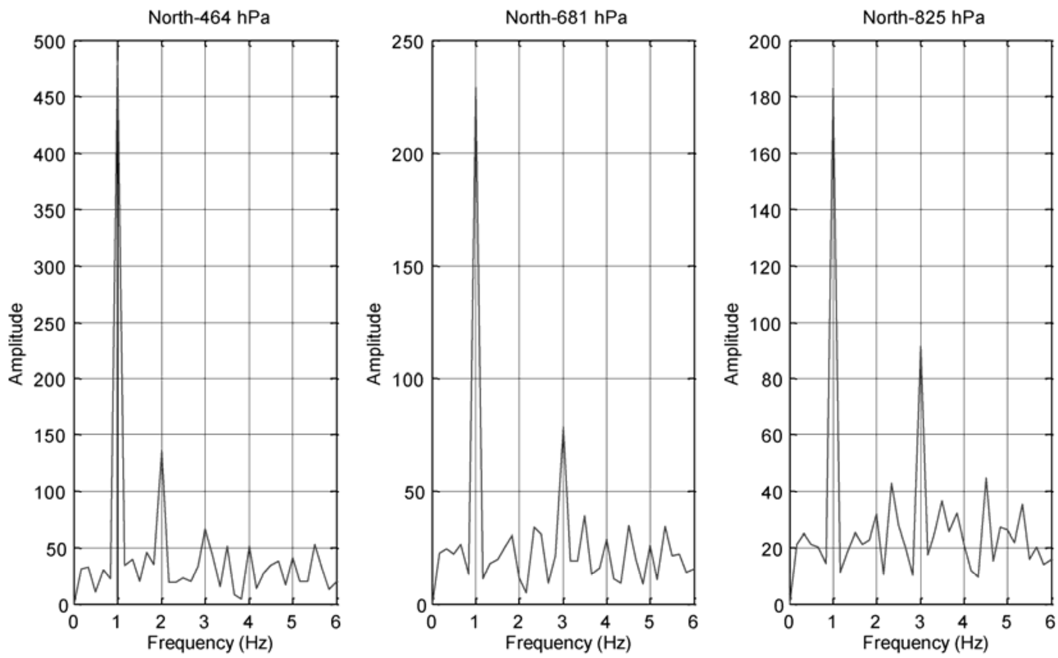

Figure 3 Frequency spectra of ozone over northern China at different pressure levels.

Table 1 TES-retrieved average ozone mixing ratios over the three Chinese regions at different pressure levels

	464 hPa	681 hPa	825 hPa
North China	68.8	63.1	61.5
South China	63.7	55.9	55.5
West China	64.1	60.0	missing

northern China. A significant signal appears at f=1 Hz at all pressure levels, which implies a constant seasonal variation throughout the troposphere. Another relatively strong signal appears at f=2 Hz at 464 hPa, and f=3 Hz at 681 hPa and 825 hPa.

The inter-annual trend of ozone is derived by performing IFFT on the 0–0.7 Hz part of the spectrum, (Figure 4). A significant increasing trend of ozone mixing ratios is observed at all three pressure levels, with the largest rate of increase at 464 hPa (0.89 ± 0.059 nL/(L a)), followed by that at 681 hPa (0.57 ± 0.065 nL/(L a)) and the smallest rate

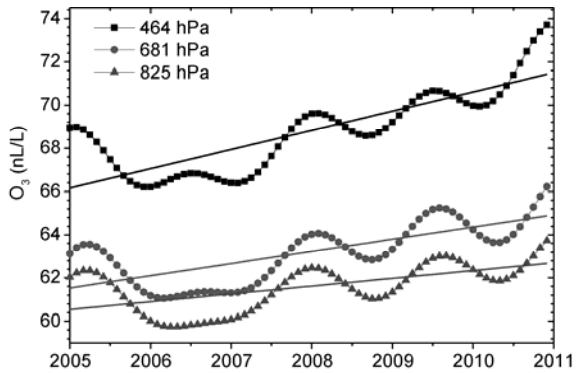

Figure 4 Inter-annual ozone trend in northern China.

at 825 hPa (0.36 ± 0.074 nL/(L a)). Higher levels are more likely to be affected by the global O_3 background and this trend also implies a fast increase of global background ozone. Surface ozone in Beijing is increasing at the rate1.1 nL/(L a) from 2001 to 2006 by analyzing the observation data in 6 stations cites [21]. This increase is higher than that from our results, and implies three possible explanations. First, our study covers a time span from 2005 to 2010, which is different from Tang's. Second, we focus on the average ozone over whole North China instead of some big cities. Third, the TES data reflects the ozone change in the lower troposphere instead of the surface atmosphere.

From the frequency spectrogram the seasonal variation is superimposed with other different cycles. If the data is filtered such that signals with amplitudes <15% of the maximum amplitude are excluded, and IFFT is performed in frequency ranges including 0.8–1.2, 0.8–2.2 and 0.8–3.2 Hz, the resulting seasonal variations obtained from IFFT get much closer to the observed variations (Figure 5). The amplitude is largest at 464 hPa, reaching −13 to 15 nL/L. A weak double-peak phenomenon is observed at 825 hPa, with peaks in spring and autumn and troughs in winter and summer.

3.2 Southern China

The results of a similar analysis for southern China appears in Figure 6. Strong signals appear at f=1, 2 and 3 Hz at all the pressure levels, with strongest at f=1 Hz.

We obtained the inter-annual trend by performing IFFT on the 0–0.7 Hz frequency range (Figure 7). A weak in

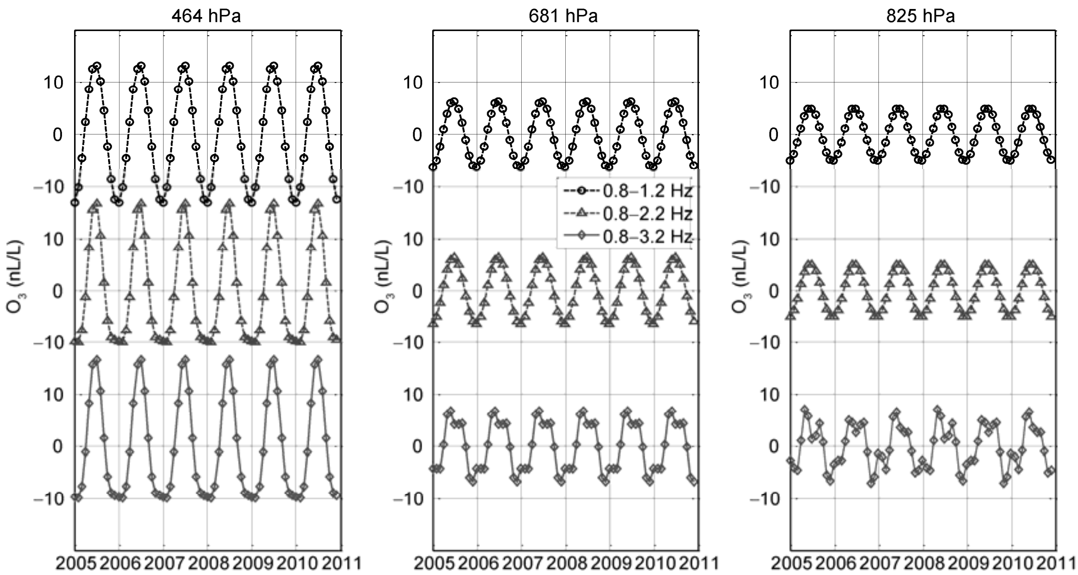

Figure 5 Seasonal variations of tropospheric ozone over northern China.

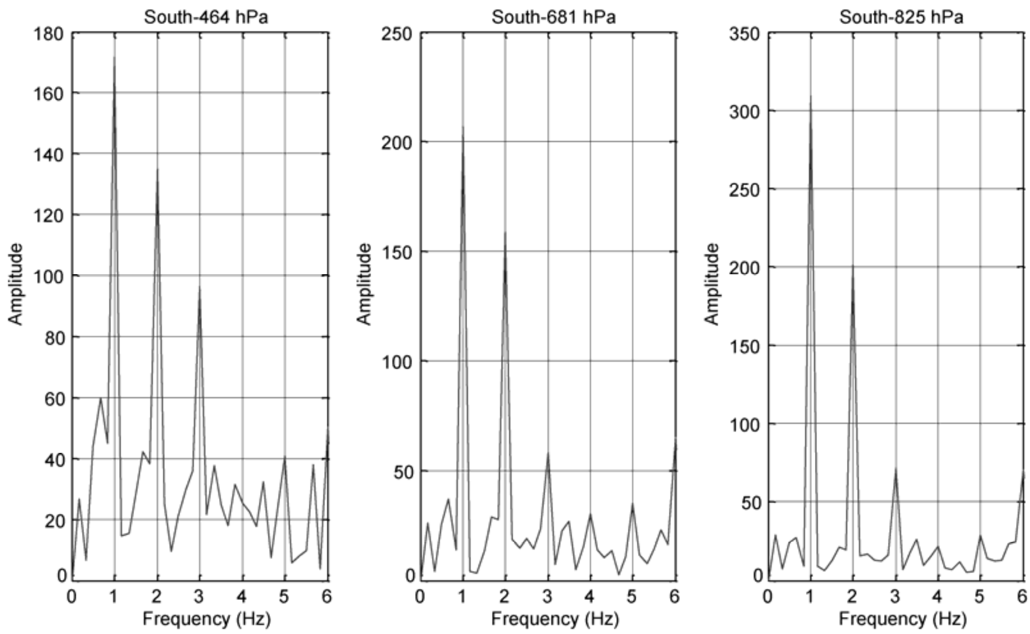

Figure 6 Frequency spectra of ozone over southern China at different pressure levels.

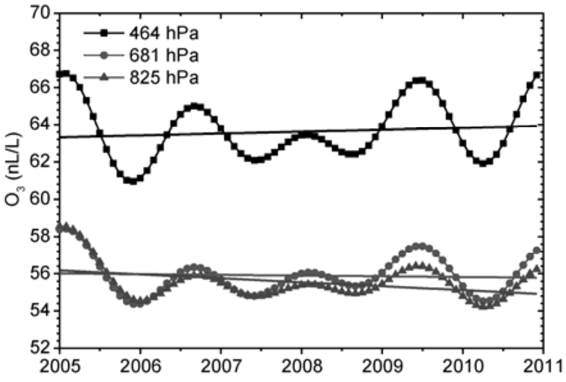

Figure 7 Inter-annual ozone trend over southern China.

creasing trend (0.10 ± 0.11 nL/(L a)) is observed at 464 hPa and a weak decreasing trend (−0.21 ± 0.061 nL/(L a)) is observed at 825 hPa. At 681 hPa, ozone concentrations remain constant over the five years (−0.04 ± 0.07 nL/(L a)). This is consistent with the results of previous work which also showed a slight decreasing trend from 1991 to 2006 in Lin'an [22].

The frequency spectra shows that the ozone seasonal variation is 3 different cycles superimposed. By filtering out signals with amplitudes < 15% of the maximum amplitude, and performing IFFT on different frequency ranges including 0.8–1.2, 0.8–2.2 and 0.8–3.2 Hz, Figure 8 show that the seasonal variations over southern China are more complex than those over northern China. A double-peaks phenomenon is significant at all three levels and O_3 displays a summer minimum. The amplitude of the seasonal change is highest at 825 hPa, reaching −15 to 10 nL/L.

3.3 Western China

The frequency spectra of tropospheric ozone over western China appears in Figure 9. A strong signal appears at f=1 Hz and a slightly weaker one at f=2 Hz at 464 hPa.

The inter-annual trend was obtained by performing IFFT on the 0–0.7 Hz signals (Figure 10). An increasing trend (+0.26 ± 0.049 nL/(L a) at 464 hPa and 0.41 ± 0.041 nL/(L a) at 681 hPa) was observed over western China.

Over western China, the seasonal change of tropospheric ozone is very regular, with summer maxima and winter minima, (Figure 11). This regularity can be explained by the dominant role of the ozone background over this region and the very small anthropogenic influence. At 464 hPa the amplitude reaches −10 to 12 nL/L, and is smaller at 681 hPa, reaching −5 to 5 nL/L.

4 Conclusions

The inter-annual trend and seasonal variations retrievedfrom TES over different regions in China is summarized in Table 2. Over the three regions, ozone mixing ratios are generally higher in summer and lower in winter. Over southern China at all three pressure levels and northern China at 825 hPa, however, ozone shows double peaks occurring in spring and autumn as a result of the combined effects of atmospheric chemistry and global transport [23]. Significant increases in ozone are found over all three regions at 464 hPa and the rate of increase is fastest over northern China, reaching 0.89±0.059 nL/(L a). At 681 hPa, ozone shows increases over northern and western China, at a rate of 0.57±0.065 nL/(L a)

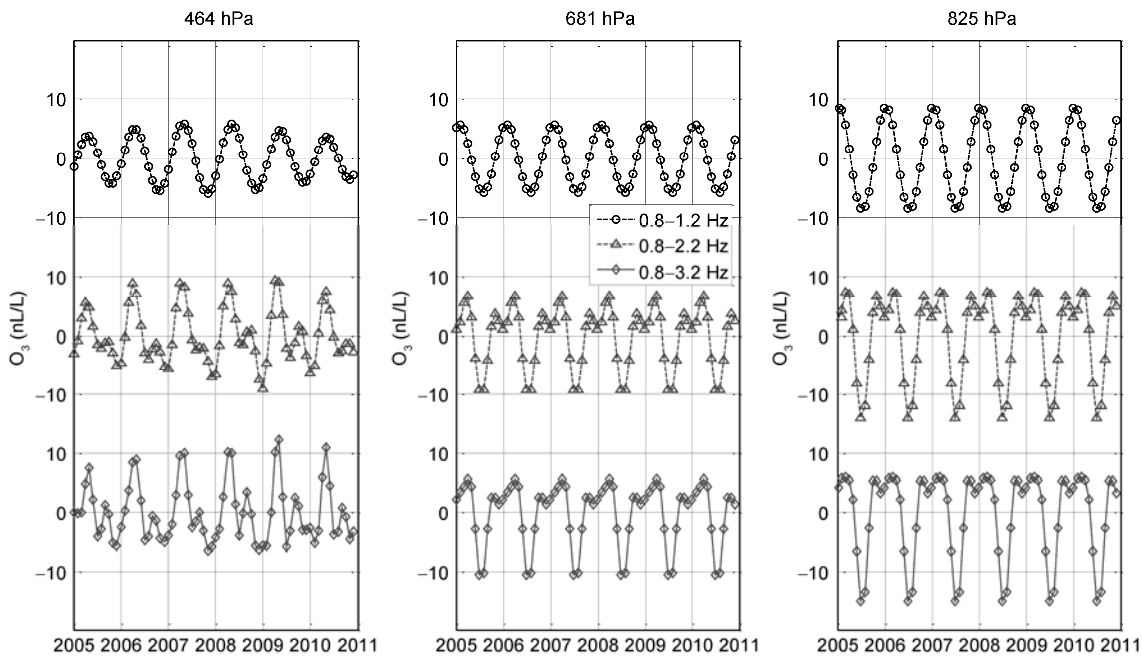

Figure 8 Seasonal variations of tropospheric ozone over southern China.

Table 2 The summary of the inter-annual trend and seasonal variations of ozone in China from 2005 to 2010

		Northern China			Southern China			Western China	
		464 hPa	681 hPa	825 hPa	464 hPa	681 hPa	825 hPa	464 hPa	681 hPa
Inter-annual trend (nL/(L a))		0.89±0.059	0.57±0.065	0.36±0.074	0.10±0.11	−0.04±0.07	−0.21±0.061	0.26±0.049	0.41±0.041
Seasonal variations (nL/L)	Features	normal (*)	normal	double peaks	double peaks	double peaks	double peaks	normal	normal
	Amplitudes	−12–15	−8–8	−8–8	−5–12	−10–6	−15–9	−10–12	−5–5

(*) refers to a general seasonal feature in China: ozone concentration is high in summer and low in winter.

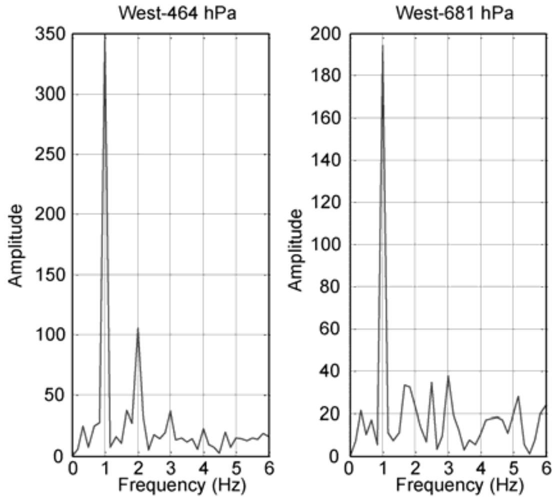

Figure 9 Frequency spectra of ozone over western China at various pressure levels.

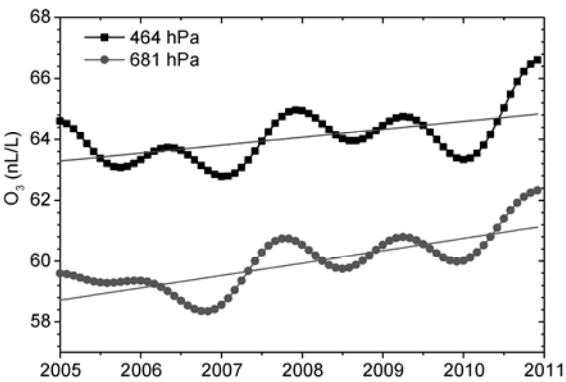

Figure 10 Inter-annual ozone trend over western China.

and 0.41 ± 0.041 nL/(L a) respectively, but is almost constant over southern China. At 825 hPa, ozone increases at a rate of 0.36 ± 0.074 nL/(L a) over northern China, while decreasing over southern China at a rate of -0.21 ± 0.061 nL/(L a).

The TES data show an overall increase in tropospheric ozone concentrations over China from 2005 to 2010, implying increasing adverse impact of tropospheric ozone on human health, agricultural activity and eco-systems. Multiple factors may contribute to this increasing trend. One

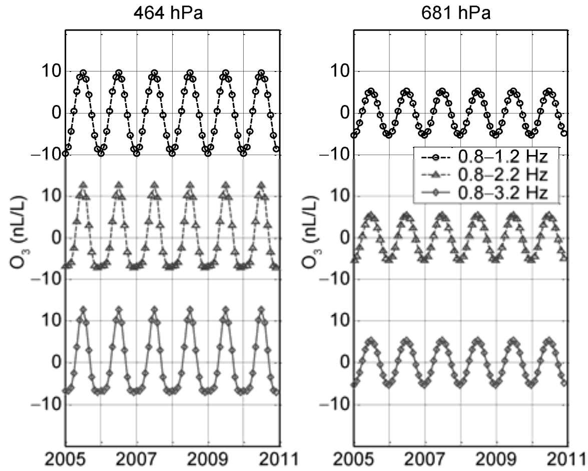

Figure 11 Seasonal variations of tropospheric ozone over western China.

reason is the rising emissions of ozone precursors, mostly over northern China. Another reason is the impact from the change in transport, including the stratosphere-troposphere ozone exchange over western China, and the monsoonal circulation in southern regions. Other natural factors, such as the climate-driven changes of soil NO_x emissions and biogenic VOCs emissions, can also contribute to the trend. This analysis provides a useful observational dataset and tools for future investigations into the mechanisms responsible for tropospheric ozone changes over China.

This work was supported by the National Natural Science Foundation of China (41005060). TES data is managed by NASA Jet Propulsion Laboratory (JPL) and we thank Dr. M. Luo at JPL for providing the TES ozone data.

1 Seinfeld J H, Pandis S N. Atmospheric Chemistry and Physics, from Air Pollution to Climate Change. New York: Wiley-Interscience Publication, 1998. 35–36
2 Wu S L, Mickley L, Leibensperger E M, et al. Effects of 2000–2050 global change on ozone air quality in the United States. J Geophys Res, 2008, 113: D06302
3 Akimoto H. Global air quality and pollution. Science, 2003, 302: 1716–1719
4 Fiore A M, Dentener F J, Wild O. Multi-model estimates of intercontinental source-receptor relationships for ozone pollution. J Geophys Res, 2009, 114, doi:10.1029/2008JD010816
5 Tang X Y, Zhang Y H, Shao M. Atmospheric Environmental Chemistry (in Chinese). Beijing: Higher Education Press, 2006.107–108

6 Richter A, Burrows J P, Nuß H, et al. Increase in tropospheric nitrogen dioxide levels over China observed from space. Nature, 2005, 437: 129–132

7 Zhang L, Jacob D J, Boersma K F. Transpacific transport of ozone pollution and the effect of recent Asian emission increases on air quality in North America: An integrated analysis using satellite, aircraft, ozonesonde, and surface observations. Atmos Chem Phys, 2008, 8: 6117–6136

8 Ding A J, Wang T, Thouret V. Tropospheric ozone climatology over Beijing: Analysis of aircraft data from the MOZAIC program. Atmos Chem Phys, 2008, 8: 1–13

9 Wang T, Wei X L, Ding A J, et al. Increasing surface ozone concentrations in the background atmosphere of Southern China, 1994–2007. Atmos Chem Phys, 2009, 9: 6217–6227

10 Zhou X J, Luo C, Ding G A, et al. The ozone and its precursors concentration change in Eastern China (in Chinese). Sci China B, 1994, 24: 1323–1330

11 Ding G A, Xu X B, Luo C, et al. Surface ozone characteristics at different areas under atmospherical background conditions in China (in Chinese). Acta Meteorol Sin, 2001, 59: 88–96

12 Zhu B, Wang T, Ni D H. Photochemical ozone and characteristics of its precursors in the boundary layer of Lin'an, a rural-agricultural site of Eastern China during 1999 autumn (in Chinese). J Nanjing Instit Meteorol, 2004, 27: 185–192

13 Liu J, Zhang X L, Zhang X C, et al. Surface ozone characteristics and the correlated factors at Shangdianzi atmospheric background monitoring station (in Chinese). Res Environ Sci, 2006, 19: 19–25

14 Boersma K F, Jacob D J, Bucsela E J, et al. Validation of OMI tropospheric NO2 observations during INTEX-B and application to constrain NO_x emissions over the eastern United States and Mexico. Atmos Environ, 2008, 42: 480–497

15 Logan J A, Megretskaia I A, Nassar R, et al. Effects of the 2006 El Nino on tropospheric composition as revealed by data from the Tropospheric Emission Spectrometer (TES). Geophys Res Lett, 2008, 35: L03816

16 Beer R. TES on the Aura mission: Scientific objectives, measurements, and analysis overview. IEEE Trans Geosci Remote Sens, 2006, 44: 1102–1105

17 Bowman K W, Rodgers C D, Kulawik S S, et al. Tropospheric emission spectrometer: Retrieval method and error analysis. IEEE Trans Geosci Remote Sens, 2006, 44: 1297–1307

18 Nassar R, Logan J A, Worden H M, et al. Validation of tropospheric emission spectrometer (TES) nadir ozone profiles using ozonesonde measurements. J Geophys Res, 2008, 113: D15S17

19 Wang Y X, Munger J W, Xu S C, et al. CO_2 and its correlation with CO at a rural site near Beijing: Implications for combustion efficiency in China. Atmos Chem Phys, 2010, 10: 8881–8897

20 Thoning K W, Tans P P, Komhyr W D. Atmospheric carbon dioxide at Mauna Loa observatory 2: Analysis of the NOAA GMCC data, 1974–1985. J Geophys Res, 1989, 94: 8549–8565

21 Tang G, Li X, Wang Y, et al. Surface ozone trend details and interpretations in Beijing, 2001–2006. Atmos Chem Phys, 2009, 9: 8813– 8823

22 Xu X, Lin W, Wang T, et al. Long-term trend of surface ozone at a regional background station in eastern China 1991–2006: Enhanced variability. Atmos Chem Phys, 2008, 8: 2595–2607

23 Wang Y X, Zhang Y Q, Luo M. Seasonal and spatial variability of surface ozone over China: Contributions from background and domestic pollution. Atmos Chem Phys, 2011, 11: 3511–3521

Open Access This article is distributed under the terms of the Creative Commons Attribution License which permits any use, distribution, and reproduction in any medium, provided the original author(s) and source are credited.